Evaluation of Total Loss for an Inverter and Motor by Applying Modulation Strategies

Jun-ichi Itoh, Takumi Ogura
Nagaoka University of Technology
Department of Electrical, Electronics and Information Engineering,
1603-1 Kamitomioka-cho,Nagaoka city Niigata, Japan,
itoh@vos.nagaokaut.ac.jp, takumi94@stn.nagaokaut.ac.jp

***Abstract*—This paper evaluates total loss of an induction motor and a permanent magnetic motor drive system applying two various modulation strategies on each motor, which are the PWM operation and the six-step operation. At first, the loss analysis is implemented based on the theoretical model of an inverter and an induction motor. As a result, when the leakage inductance is less than 25%, the PWM drive should be used instead of six-step operation in order to obtain the minimum loss. On the other hands, when the leakage inductance is more than 65%, the six-step operation is suitable for obtaining high efficiency. Additionally, an optimization point of the switching frequency is mentioned according to the leakage inductance. The validity of the loss analysis is confirmed by simulation and experimental results in which an induction motor of 1.5kW was used. Similarly, the total loss of the permanent magnet motor drive system is calculated based on the same method. When the synchronous reactance of the motor is lower than 26%, the total loss of the PWM with a 5kHz carrier is lower than the six-step modulation. On the other hands, when the synchronous reactance of the motor is more than 26%, the total loss of the six-step modulation is smaller than the PWM with a 5kHz carrier.**

***Keywords*— Inverter loss, Six-step modulation, PWM drive, Motor loss**

I. INTRODUCTION

In recent years, motor drive systems are used in many applications, such as trains, hybrid electric vehicle (HEV), home appliances and industrial system. The power consumption by motors occupies more than 50% of the total amount of the power consumption. Therefore, it is very important to improve the motor drive system efficiency in consideration of energy saving and suppression of CO_2 emission.

In order to achieve energy saving in recent years, inverters are widely applied to industry applications and home appliance. According to the applications, the modulation strategy of the inverter chooses either a six-step modulation or pulse width modulation (PWM). For example, the six-step modulation is used in trains and HEV. The six-step modulation can reduce the switching loss of the inverter because the number of the switching times is only six in per output period. Additionally, a larger output voltage can be obtained in comparison to the PWM; however the motor loss will be increased because the output voltage contains many low frequency harmonics components the 5^{th} and 7^{th} order of output frequency. These harmonics current increases the motor loss. It is noted that the harmonics current generates ripple in torque, however the amount of ripple does not contribute to increase average torque.

On the other hand, the PWM is extensively used in home appliances and industrial drives. The sinusoidal output current is obtained and the output current is controlled by an auto current regulator (ACR). Since the harmonics components in the output voltage are higher than the output frequency, the copper loss and torque ripple of the motor can be reduced by the six-step modulation. However, in PWM drive the inverter loss is larger than the six-step modulation because the switching frequency of the inverter is higher than the six-step modulation. There is a trade-off relationship between the inverter loss and the motor loss according to the modulation strategies and its switching frequency.

There are many analyses about the losses among inverter, induction motor and permanent magnetic motor regarding to efficiency [1-3]. Almost all studies discussed the motor structure and losses by using the finite element method (FEM). The FEM can easily understand the behavior of flux in the motor. Then, the best modulation strategy will be decided for each motor based on the FEM. However, when the motor parameter has changed, this process needs to be repeated to find out the best modulation strategy again. Therefore, it is difficult to discuss the best modulation strategy based on only the FEM.

This paper discusses the most suitable modulation strategy for the inverter in order to obtain a high efficiency in the inverter and the motor. The aim of this paper is to optimize the modulation strategy in the inverter according to the motor parameter. The model of the theoretical loss calculation of the inverter and motor are provided, respectively.

At first, this paper describes the inverter loss and the induction motor loss based on the theoretical model. Second, the harmonics components in the output voltage of the inverter are calculated. After that, the losses of the harmonic components are calculated by an equivalent circuit of the motor. Then, the relations between the motor parameters and the total loss are being clarified. The motor loss, which is caused by the harmonics components, is dominated by a leakage inductance L_σ of the induction motor. Therefore, the modulation strategy is chosen according to the leakage inductance of the induction motor. Note that in a PM motor the synchronous reactance will dominate the current harmonics. The calculation results are confirmed by the simulation and the experimental results with using a 1.5 kW induction motor. Finally, the permanent magnet motor losses are calculated in a similar manner. The copper loss of the PM motor is calculated by the equivalent circuit of the motor. The iron loss of the permanent magnet motor is calculated by FEM in order to make a loss table. The motor loss which is generated by the harmonics components is dominated by a synchronous reactance L_a of the PM motor.

II. LOSS ANALYSIS METHOD

A Loss analysis of an inverter

Inverter losses consists of the switching loss generates while switches are turned on and off, and the conduction loss is generated by saturation voltage of a switching device.

Figure 1(a) shows a waveform of the current and voltage in a switching device while the switch is turned on and off. If the switching pattern of the device is ideal, then the voltage and current interchange with each other instantaneously. However, the voltage and current interchange slowly as shown in Figure 1(a). That period is considered as the switching loss which is proportional to the shaped area in Figure 1(a). The switching loss P_{sw} is obtained by (1) using turn-on loss P_{on} and turn-off loss P_{off}.

$$P_{sw} = P_{on} + P_{off} \quad (1)$$

The turn-on loss P_{on} and the turn-off loss P_{off} are obtained by (2) and (3), which multiplied by turn-off E_{off}, or turn-on E_{on} and the switching frequency f_s from the data sheet of the switching device.

$$P_{on} = E_{on} \times f_s \quad (2)$$

$$P_{off} = E_{off} \times f_s \quad (3)$$

Figure 1(b) shows a current behavior in the switching device that regards to the conduction loss P_{con}. The conduction loss P_{con} can be separated into two losses P_{IGBT} and P_{FWD}, which are generated either by a switching device or a free wheel diode (FWD) according to the current direction. The conduction loss P_{con} is obtained by

$$P_{con} = P_{IGBT} + P_{FWD} \quad (4)$$

The conduction loss P_{IGBT} of a switching device and conduction loss P_{FWD} from a FWD are obtained respectively by

$$P_{IGBT} = I_p \times V_{CE} \times \left(\frac{1}{8} + \frac{m_i}{3\pi} \cos\theta \right) \quad (5)$$

$$P_{FWD} = I_p \times V_F \times \left(\frac{1}{8} - \frac{m_i}{3\pi} \cos\theta \right) \quad (6)$$

where V_{CE} and V_F are the saturation voltage of IGBT and FWD, which are obtained from a data sheet, m_i is the modulation index, $\cos\theta$ is the load power factor and I_p is the peak value of the load current. Equations (4) and (5) indicate that the switching frequency is not an element will affect on the conduction loss of IGBT and FWD.

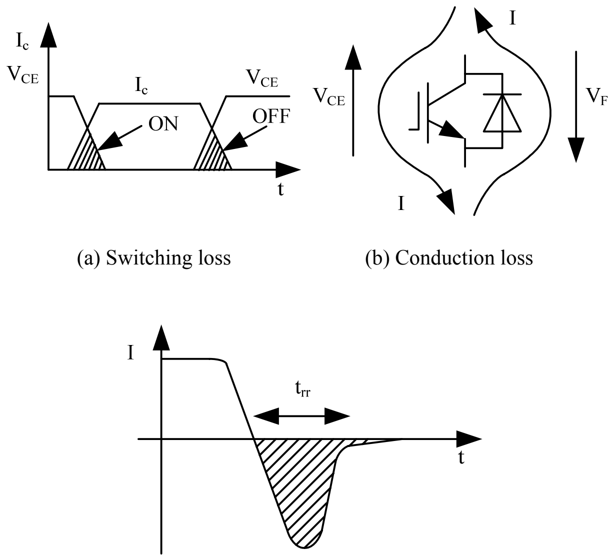

(a) Switching loss (b) Conduction loss

(c) Recovery loss

Fig. 1. Inverter loss.

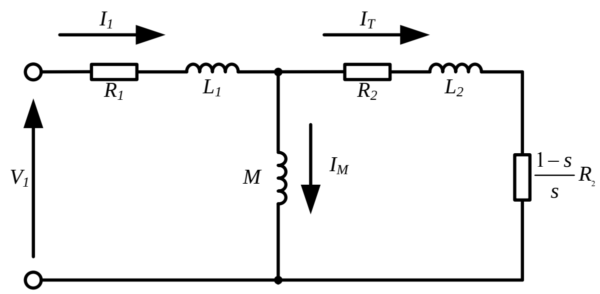

Fig. 2. Equivalent circuit of an induction motor verified by the fundamental component.

Figure 1(c) shows the recovery current in a FWD. When an IGBT is turned on, a counter FWD, which is located in a opposite side arm, becomes reverse bias. Then, the reverse recovery current occurs in the diode and a recovery loss is generated. The recovery loss of FWD is obtained by

$$P_{re} = \frac{1}{8} \times I \times V_{dc} \times t_{rr} \times f_s \quad (7),$$

where I is the RMS value of the load current, reverse t_{rr} is the recovery time, which are obtained from a data sheet, V_{dc} is the DC link voltage of inverter.

B Verification of Copper loss by the fundamental component of a motor current

Figure 2 shows a one-phase T type equivalent circuit of an induction motor. The motor loss consists of copper loss and iron loss. This paper mainly considers the copper loss according to the different modulation strategies because the iron loss in an induction motor does not depends on the modulation strategies as discussed in [1]. The copper loss is calculated by the fundamental component as follows,

$$P_1 = R_1 I_1^2 + R_2 {I_T}^2 \quad (8)$$

where R_1 is the primary resistance, R_2 is the secondary resistance, I_1 is the fundamental component of the load current of the inverter and I_T is the torque component current.

C Verification of Copper Loss by the harmonics components

The harmonic components are contained in the output voltage when the six-step modulation or PWM is used. As a result, loss is occurring in the induction motor because of containing the harmonic components.

Figure 3 shows a one-phase harmonic component equivalent circuit of an induction motor. The frequency of the harmonic components is higher than the output frequency. Therefore, slip and exciting current can be neglected in the harmonic component equivalent circuit. In addition, the impedance of the motor is dominated by the leakage inductance L_σ. Then the n-order harmonics current I_n is obtained by

$$I_n = \frac{V_n}{\omega_n L_\sigma} \quad (9),$$

where V_n is the n-order harmonic voltage in the inverter output and ω_n is the n-times angler frequency of the inverter output.

The copper loss by the harmonic current are obtained by

$$P_n = (R_1 + R_2) I_n^2 \quad (10).$$

III. QUANTIFICATION OF TOTAL LOSS

In this chapter, the optimization of the modulation strategy is clarified for the use in an induction motor. At first, in order to calculate the harmonic components of the output voltage, the six-step waveform and the PWM waveform are implemented with the Fourier series expansion. Next, the harmonic voltage is calculated, and the copper loss is calculated based on the harmonics current according to (10). Then, the converter loss, which consist of the switching loss and the conduction loss according to (1), (4) and (7), is calculated. Besides, the total loss of the inverter and the motor are obtained from each of the modulations. Finally, the leakage inductance and total loss are normalized by the motor rating. Then, the relations between the leakage inductance and the modulation strategy can be clarified.

Fourier series expansion of the output voltage from using a six-step modulation waveform is obtained by (11). The amplitude V_n of each harmonics voltage is given by (12).

$$E_n = \frac{4\sqrt{2}E_{dc}}{n\pi} cos\left(n\frac{\pi}{6}\right) \times \frac{1}{2} \quad (11)$$

$$V_n = \frac{2\sqrt{2}E_{dc}}{n\pi} \quad (12)$$

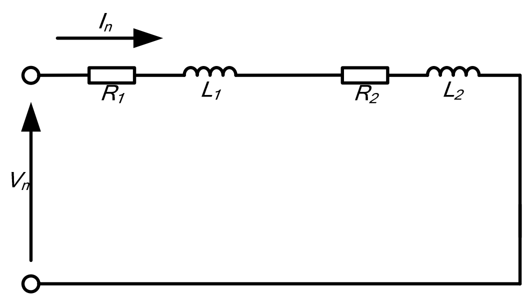

Fig.3. Equivalent circuit of an induction motor verified by harmonic components.

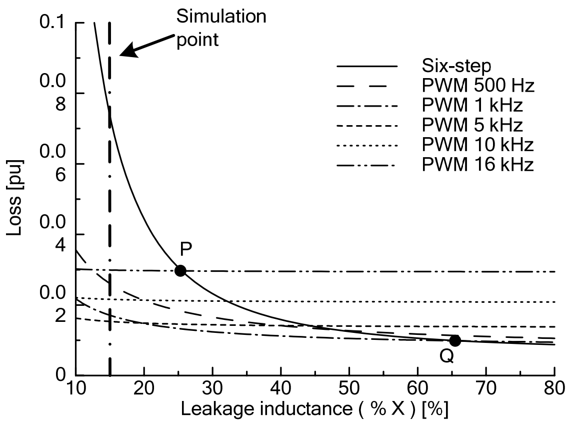

Fig. 4. Relations between the loss and the leakage inductance.

where E_{dc} is DC link voltage of the inverter.

On the other hand, Fourier series expansion in the PWM waveform is obtained by (13). Likewise, the amplitude of each harmonics voltage is obtained by (14).

$$\frac{e_M(t)}{E} = a\,cos(\omega_s t + \alpha) + \sum_{n=1}^{\infty} \frac{4}{n\pi} sin\left[\left(\frac{n\pi}{2}\right) \cdot \{a\,cos(\omega_s t + \alpha) - 1\}\right] cos\, n\omega_r t \quad (13)$$

$$V_n = \left(\frac{4E_{dc}}{n\pi}\right) J_k \left(\frac{n\pi a}{2}\right) \begin{array}{l} n = 1,3,5\ldots \quad k = 0,2,4\ldots \\ n = 2,4,6\ldots \quad k = 1,3,5\ldots \end{array} \quad (14)$$

where, J_k is the n-order Bessel function.

Eq. (9) can obtain the harmonics current by knowing the harmonics voltage. Then the equation (9) is normalized by the rated voltage, rated current and rated angler frequency of the motor, the n-order or the normalized current I_n is expressed by

$$I_n = \frac{V_n}{n\%X} \quad (15)$$

where $\%X$ is the normalized reactance of the induction motor.

From (1)-(6), the conduction loss and the switching loss are proportional to the RMS value of the current, and the switching loss is proportional to the switching frequency. Therefore, proportionality coefficients are introduced to the conduction loss and the switching loss for simplification. Using these coefficients, the total loss including inverter loss is obtained by (16) substituting (15) for (10).

$$P = 3R\sum\left(\frac{V_n}{nX}\right)^2 + (k_{con}V_{con} + k_s f_s)\sqrt{\sum\left(\frac{V_n}{nX}\right)^2} \quad (16)$$

where, n is the harmonics order(n = 1, 5, 7, 11, 13…), k_{con} is the coefficient of the conduction loss calculated by (4), k_s is the coefficient of the switching loss calculated by (1) and (7).

Figure 4 shows the relations between the losses and the leakage inductance, which is obtained by (16). Note that the calculation results are normalized with the motor parameters in Table 1. In addition, the fundamental voltage of the six-step modulation is set to rated voltage of the motor. The DC link voltage of the inverter using the PWM is set to the peak voltage of the rated phase voltage of the motor.

In figure 4, the point P is a boundary point between the switching frequency of 16 kHz and a six-step modulation. When the leakage inductance of the motor is lower than 25%, the total loss of the PWM with a 16-kHz carrier is lower than the six-step modulation. In contrast, the point Q is a boundary point between the switching frequency of 500 Hz and the six-step modulation. When the leakage inductance of the motor is more than 65%, the total loss of the six-step modulation is smaller than that of the PWM with 500-Hz carrier. That is, when the leakage inductance is small, the total loss is dominated by the motor loss because each harmonics current is increased.

The suitable modulation strategy is obtained by (17) and (18) substituting losses of the point P and the point Q into (16), which are 0.03p.u. and 0.01p.u., respectively. The conditions for which the PWM drive system is suitable are obtained by (17).

$$\%X < \frac{6R\sum(V_n/n)^2}{-(k_{con}V_{con}+k_s f_s)\sqrt{\sum(V_n/n)^2}+\sqrt{\{k_{con}V_{con}+k_s f_s\}^2\sum(V_n/n)^2+\left(0.36R\sum(V_n/n)^2\right)}} \tag{17}$$

$$\%X > \frac{6R\sum(V_n/n)^2}{-(k_{con}V_{con}+k_s f_s)\sqrt{\sum(V_n/n)^2}+\sqrt{\{k_{con}V_{con}+k_s f_s\}^2\sum(V_n/n)^2+\left(0.12R\sum(V_n/n)^2\right)}} \tag{18}$$

The PWM is better than the six-step modulation when the leakage inductance is constrained by (17). Likewise, the six-step modulation is better than the PWM when the leakage inductance is constrained by (18).

IV. VERIFICATION OF THE LOSS ANALISYS BASED ON SIMULATION AND EXPERIMANTAL RESULTS

A Simulation verifications

At first in order to evaluate the validity of Figure 4, loss analyses for the motor and inverter were simulated. Table 1 shows the parameters of an induction motor. The simulation condition, where $\%X$ = 14.7%, is used.

Figure 5 shows a relationship between the total loss and the switching frequency. The simulation conditions are shown in Table 1. From the results, the copper loss of the induction motor becomes larger when the switching frequency is lower because the large low-order harmonics components are contained in the motor current. In contrast, when the switching frequency is higher, the inverter loss is increased because of higher switching loss is occurring. As a result, the total loss is reducing to a minimum at PWM 5kHz where the motor loss is decreasing to balance with the increased inverter loss.

TABLE I. PARAMETERS OF INDUCTION MOTOR

Items	Values
Rated power	1.5kW
Phases and poles	3phases, 4poles
Rated frequency	51Hz
Rated voltage	188V
Rated current	7A
Rated speed	1500r/min
Primary resistance R1	1.09Ω
Secondary resistance R2	0.79Ω
Leakage inductance L□	7.29mH
Mutual inductance Lm	85.3mH
Moment of Inertia	0.009kg m2

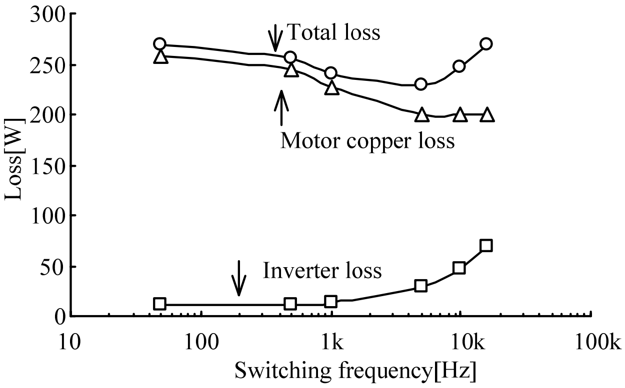

Fig. 5. Relations between the loss and the switching frequency.

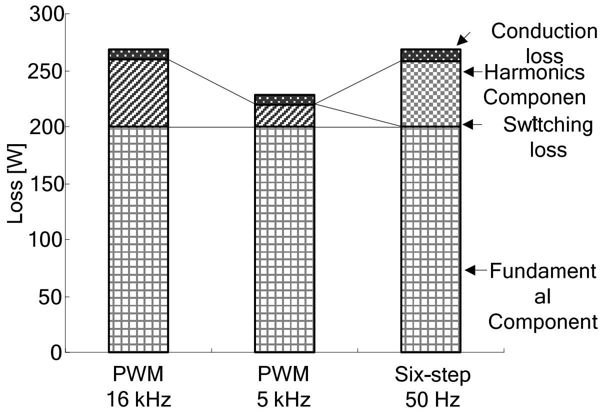

Fig. 6. Loss comparison for various modulation strategies.

Figure 6 shows the loss comparison among various modulation strategies. The harmonics loss in the motor is increased by the six-step modulation. Thus, the total loss is increased. On the other hand, the PWM with 16-kHz carrier generates little loss depending on harmonics component though the switching loss of the inverter increases. As a result, the switching frequency of 5 kHz is optimal modulation strategy for the motor as shown in Table 1.

B Experimental verifications

The total loss was evaluated by experimental results using the induction motor of Table 1. The vector control is used in PWM in order to keep the same current without any compensation for the dead time voltage error. It is noted that the V/f control is used in six-step modulation; however the fundamental voltage of the inverter output is set to the same as other conditions.

Figure 7 shows the output voltage and current waveform of the six-step modulation. The output current has large distortion due to the six-step modulation. The total harmonic distortion (THD) of the output current is 62.9 %.

Figure 8 show the harmonics analysis results of the six-step modulation. The harmonic components of 5th and 7th order are appeared largely. The average torque is not increased by these harmonic components because the harmonic current generates torque ripple of 6th order in the output frequency.

Figure 9 shows the output voltage and current waveforms using the PWM with a 16-kHz carrier. The motor current becomes a sinusoidal waveform by using the PWM. The THD of the motor current is 2.59 %. Likewise, when the switching frequency of 5kHz is used the motor current can obtain a sinusoidal waveform as well.

Figure 10 shows the harmonics analysis results of PWM with a 16-kHz carrier. Since the current feedback is applied in vector control, the output current contains few of the low-order harmonics components.

Figures 11 (a) and (b) show the losses about the inverter and motor at 50% and 25 %load condition, respectively. The minimum total loss is obtained when the switching frequency is 5 kHz. This result well agrees with the simulation result. It is noted that the loss in the experimental results is different from the simulation because of the iron loss of tan induction motor is

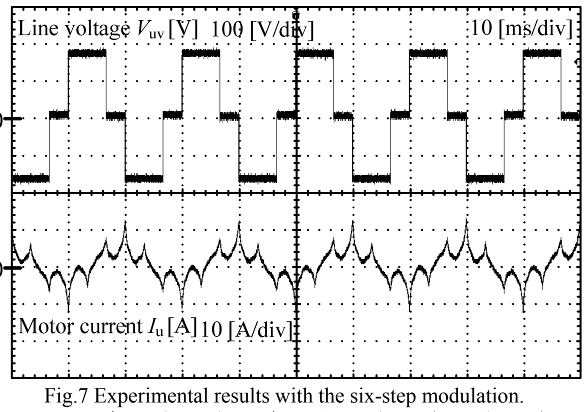

Fig.7 Experimental results with the six-step modulation.

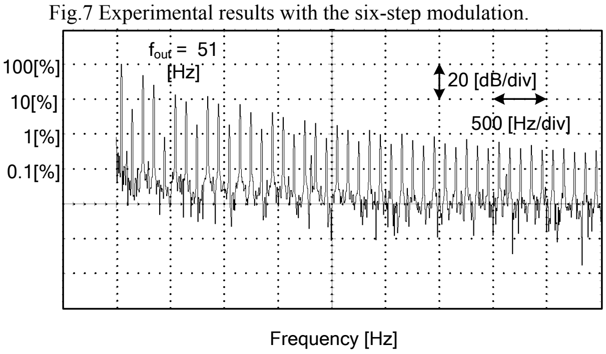

Fig. 8. Harmonics analysis results of the six-step modulation.

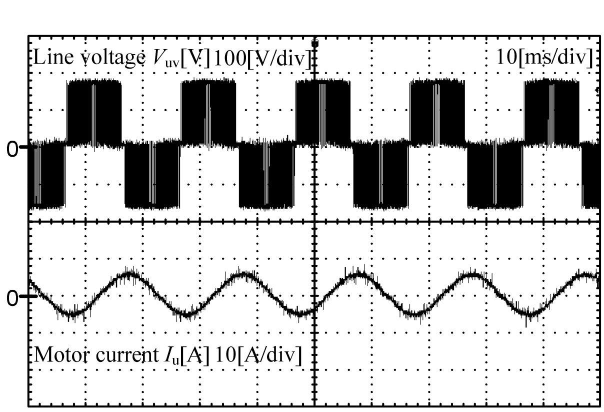

Fig. 9 Experimental results using the PWM with a 16-kHz carrier.

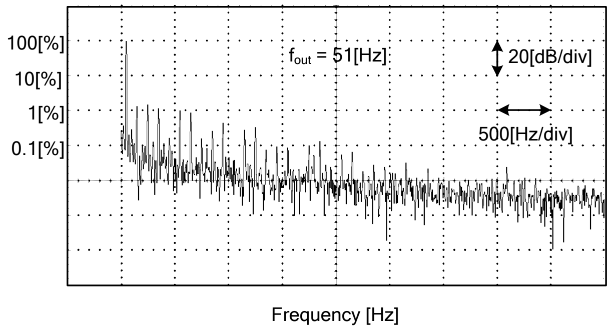

Fig. 10. Harmonics analysis results using the PWM with a 16-kHz carrier.

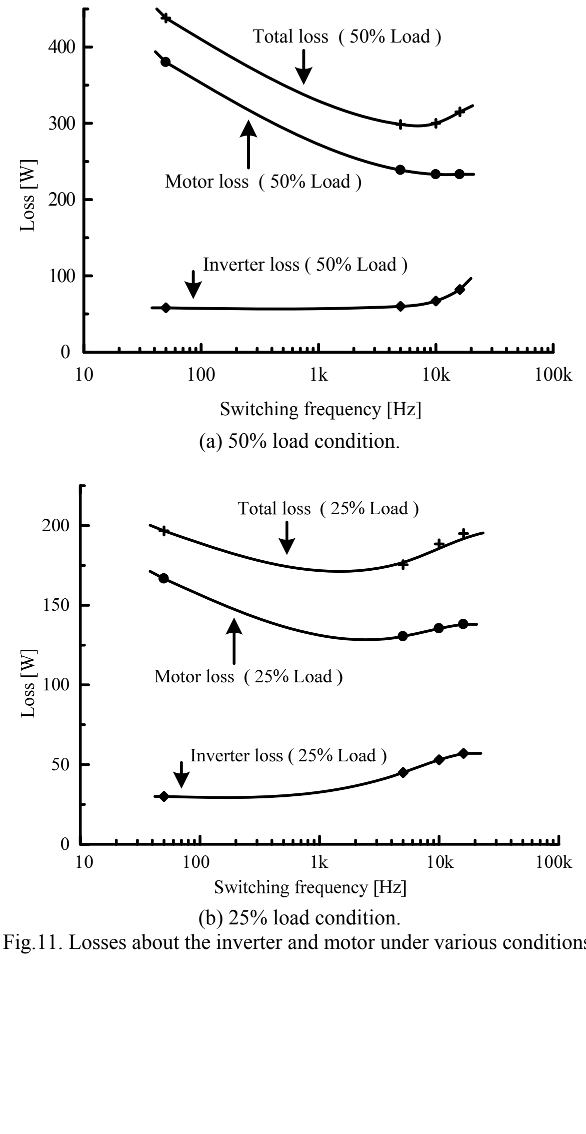

(b) 25% load condition.

Fig.11. Losses about the inverter and motor under various conditions.

neglected in the simulation analysis.

Then, the modulation is optimized by considering to the motor characteristic. When the leakage inductance is less than 25%, the PWM should be used in order to obtain the minimum loss. On the other hands, when the leakage inductance is more than 65%, the six-step modulation is suitable to obtain the highest efficiency. From this, since the leakage inductance of a general purpose induction motor is approximately 10%-20%, the PWM is suitable for its drive. On the other hand, the advantage of the six-step modulation is appeared in the motor, which has high fundamental frequency, small primary and secondary resistance, and a large leakage inductance. That is, for a high speed motor that has large normalized leakage reactance, is suitable for the six-step modulation.

V. LOSS ANALYSIS OF PERMANENT MAGNET MOTOR

A Verification of Copper loss by the fundamental component of the motor current

Table 2 shows the parameters of a permanent magnet motor that used as an example in this paper. It is noted that the inverter loss analysis was evaluated by the same method as discussed in Chapter II.

Figure 12 shows a single-phase equivalent circuit of a PM motor. The motor loss composed of the copper loss and the iron loss. The copper loss of the permanent magnet motor is calculated by the fundamental component of the motor as shown in (19).

$$P_1 = R_a I_1^2 \quad (19)$$

where R_a is a winding resistance, I_1 is a fundamental component of the load current of the inverter.

B Copper loss by the harmonics components

The harmonic voltage is applied to the PM motor when the six-step modulation and the PWM are applied. As a result, the loss which is caused by the harmonic components occurs in the permanent magnet motor.

Figure 13 shows the single-phase equivalent circuit of a PM motor for high frequency components. The back electromotive force is disappeared in the equivalent circuit because the back electromotive force does not contain high frequency components. The impedance of the motor is dominated by the synchronous reactance L_a from figure 13. Then the n-order harmonics current I_n is obtained by

$$I_n = \frac{V_n}{\omega_n L_a} \quad (20),$$

where V_n is the n-order harmonic voltage of the inverter output voltage and ω_n is the n-times natural angular frequency of the inverter output.

The copper loss is calculated based on the harmonic current is obtained by

$$P_n = R_a I_n^2 \quad (21),$$

C Iron loss analysis by FEM

The iron loss of the permanent magnet motor occurs in the stator, the rotor and the magnet. An eddy current loss

TABLE II. PARAMETERS OF PERMANENT MAGNET MOTOR

Items	Values
Rated power	1.5kW
Phases and poles	3phases, 6poles
Rated frequency	90Hz
Rated voltage	180V
Rated current	6.1A
Rated speed	1800r/min
Back electromotive force	147V
Winding resistance R_a	0.783Ω
Synchronous reactance L_a	11.5mH
Number of poles	36slots
Stator outer diameter	130mm
Stator inner diameter	83mm
Winding configuration	138turn,series per phase
Rotor outer diameter	82.2mm
Rotor shaft diameter	30mm
Electrical resistivity ρ (magnet)	1.4×10^{-6}Ωm

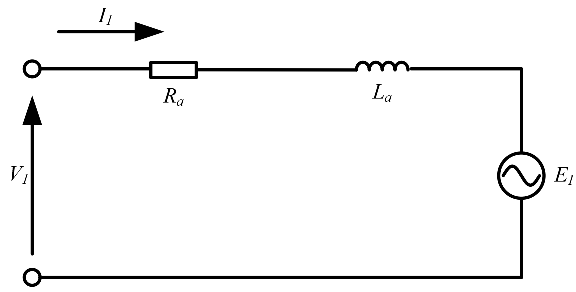

Fig 12 Equivalent circuit of a PM motor verified by the fundamental component.

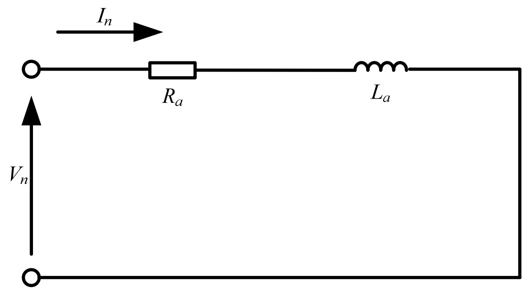

Fig 13 Equivalent circuit of a PM motor verified by the harmonic components.

in the magnet is changed largely by the switching frequency. Therefore, the eddy current loss should be analyzed by a simplified model using mathematics equation; however the eddy current loss in the magnet is changed by the motor shape. That is, it is difficult to analysis only mathematic model. Therefore, in the first step, the analysis using FEM is introduced for the eddy current loss analysis in this chapter.

Figure 14 shows a motor model by using FEM. The specification of the magnet is shown in Figure 14 and Table 2. Internal magnet motor (IPM) of 1.5kW, 180V is selected as one of example. The number of pole is 6. This motor is used for industrial applications in 200V-power grid lines.

Figure 15 shows the current density of the magnet for each of the input voltage waveforms. The current density in the sinusoidal wave drive, which is an ideal condition, is distributed equally. On the other hands, in the six-step modulation and the PWM with a 450Hz carrier, a current density becomes greatly higher than the other modulation conditions. That is, the current density of the PM motor becomes larger when the switching frequency is lower because the low order harmonics components of the motor are becoming larger.

Figure 16 shows the loss from the eddy current by using FEM analysis. From the results, we know that the eddy current loss of the PM motor is proportional to the current density, therefore the loss becomes larger when the switching frequency is lower.

Figure 17 concludes the relations between the eddy current loss and the synchronous reactance. The eddy current loss for each of the modulation strategies was analyzed by the FEM according to various values of synchronous reactance. The eddy current loss of FEM result is approximated by

$$P_e = aX^{-b} \qquad (22),$$

where a and b are the constant parameters, which are fitting according to each simulation results. Table 3 shows the constant parameter a and b for each results. The eddy current loss is estimated under various conditions by (22) with Table 3.

VI. Quantification of Total loss

In order to discuss which of the modulation strategy is best for the PM motor, first the motor loss needs to quantify according to the modulation strategy. The six-step drive waveform and the PWM drive waveform is implemented with the Fourier series expansion to obtain the harmonic component of the inverter output. As a result, the harmonic voltage and current are obtained, respectively. Then, the copper loss is calculated from the harmonics current according to (21). After that, the eddy current loss is calculated by (22), and the total loss of both the inverter and the motor is sum-up from each various modulation. Finally, the synchronous reactance and the total loss are normalized by the motor rating. Then, the relations between the synchronous reactance and the modulation strategy are clarified.

As discussed in the previous chapter, Fourier series expansion of the inverter output voltage using a six-step modulation waveform is obtained by (11). The amplitude V_n of each harmonics voltage is given by (12). In addition, Fourier series expansion of the PWM waveform is obtained by (13). Therefore, the amplitude of each harmonics voltage is obtained by (14).

The harmonics current which is generated by each harmonics voltage is obtained by (20). When the equation (20) is normalized by the rated voltage, current, angler frequency of the motor and the n-order normalized current I_n is obtained by (15).

The total loss is quantified by the expression of the loss. From (1)-(6), the conduction loss and the switching loss are proportional to the RMS value of the current; the switching loss is proportional to the switching frequency. Therefore, the proportionality coefficient k_{con} and k_s are introduced to the conduction loss and the switching loss, respectively. The copper loss of the motor is obtained by

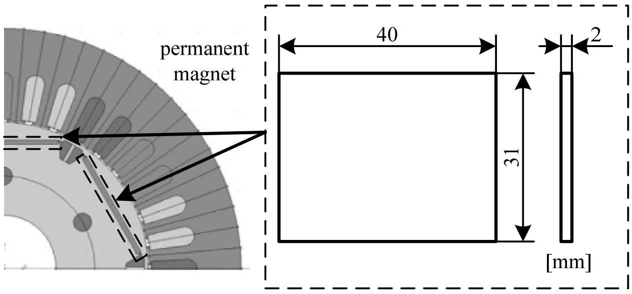

Fig. 14. The model of a FEM motor.

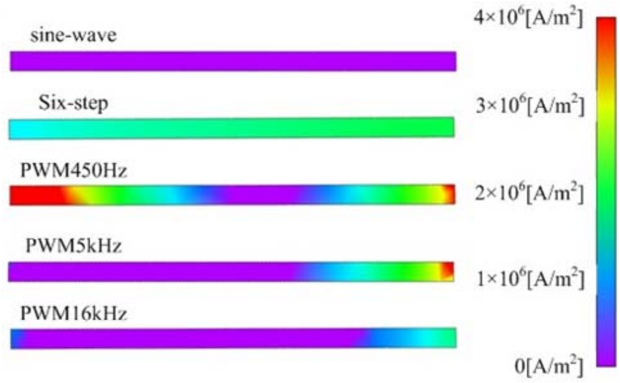

Fig. 15. Magnetic current density.

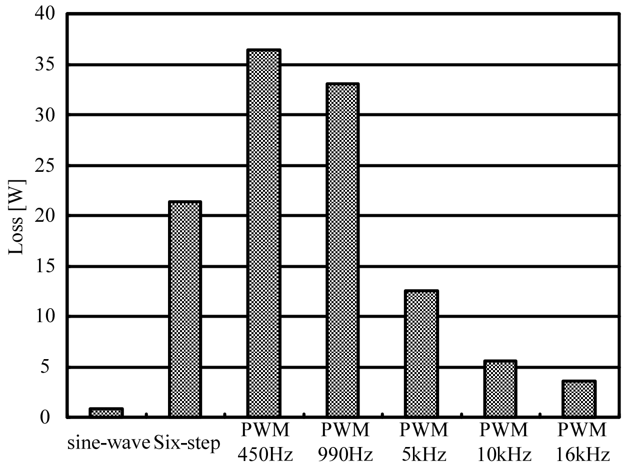

Fig. 16. Eddy current loss by the FEM analysis.

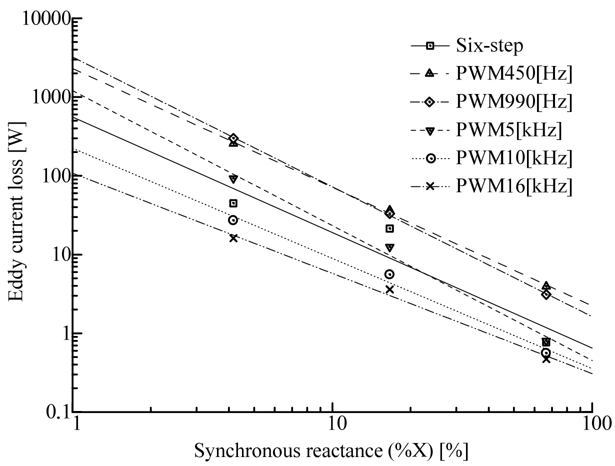

Fig. 17. Relations between the eddy current loss and the synchronous reactance

substituting (15) in (19). In addition, the eddy current loss of the motor is obtained by (22). The total loss which consists of the inverter loss, the copper loss of the motor and the eddy current loss of the motor can be obtained by

$$P = 3R_a \sum \left(\frac{V_n}{nX} \right)^2 + (k_{con}V_{con} + k_s f_s)\sqrt{\sum \left(\frac{V_n}{nX} \right)^2} + aX^{-b} \quad (23).$$

Figure 18 shows relations between the loss and the synchronous reactance, which is obtained by (23). Note that the calculation results are normalized with the motor parameters in Table 2.

In figure 18, the point Q is the boundary point between the PWM drive with a 5kHz carrier and the six-step modulation. When the synchronous reactance of the motor is lower than 26%, the total loss of the PWM with a 5kHz carrier is lower than the six-step modulation. On the other hands, when the synchronous reactance is more than 26%, the total loss of the six-step modulation is smaller than the PWM with a 5kHz carrier. The copper loss of the PM motor is lower than the induction motor because PM motor does not contain the secondary resistance. In the case of synchronization reactance is about 30%, the eddy current loss is almost equally on all the control strategies. Therefore, the range which is suitable for the six-step drive expands in comparison to that of the induction motor.

VII. Conclusion

This paper described the total loss among the inverter loss, the induction motor and PM motor. The motor loss and the inverter loss are calculated by simple equations. Besides, the optimization of modulation strategy for the inverter is clarified.

As a result, when the leakage inductance in the induction motor is less than 25%, the PWM should be used in order to obtain the minimum loss. On the other hands, when the leakage inductance is more than 65%, the six-step modulation is suitable to obtain highest efficiency. The total loss is at minimum for a 1.5-kW general purpose induction motor when the switching frequency is 5 kHz on the PWM drive. The simulation and experiment results confirmed the validity of the theoretical analysis.

On the other hands, when the synchronous reactance in the PM motor is lower than 26%, the total loss of the PWM with a 5kHz carrier is lower than the six-step modulation. When the synchronous reactance is more than 26%, the total loss of the six-step modulation is smaller than the PWM with a 5-kHz carrier.

In future study, the iron loss will be considered and the optimization of the modulation strategy PM motor will be discussed in the term of experiment.

TABLE III. The constant number of each input waveform

Input waveform	a	b
Six-step	560	1.5
PWM450Hz	2300	1.5
PWM990Hz	3200	1.6
PWM5kHz	1200	1.7
PWM10kHz	220	1.4
PWM16kHz	110	1.3

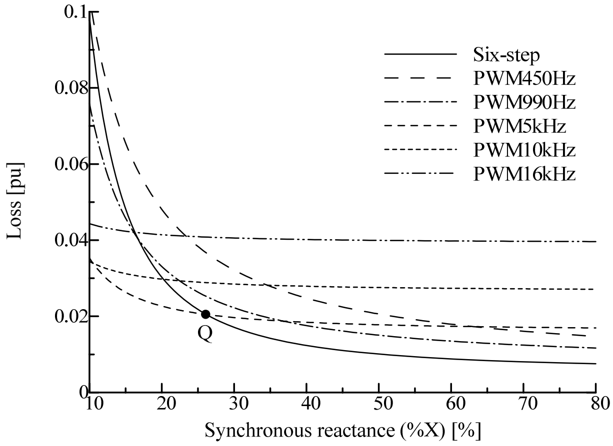

Fig 18 Relations between the loss and the synchronous reactance.

References

[1] K. Yamazaki, Y. Seto and M. Tanida: "Iron Loss Analysis of IPM Motor Considering Carrier Harmonics", IEEJ Trans., Vol.125-D, No.7, pp.758-766 (2005) In Japanese.

[2] K. Yamazaki and A. Abe: "Loss Analysis of IPM Motors Considering Carrier Harmonics –Calculation of Eddy Current Loss in Permanent Magnet Using 3-D Finite Element Method–", IEEJ Trans., Vol.127-D, No.1, pp.87-94 (2007) In Japanese.

[3] K. Yamazaki and N. Fukushima: "Carrier Loss of Induction Motors Driven by Inverters –Comparison between Results Separated by Experiment and Field Analysis–", IEEJ Trans., Vol.129-D, No.11, pp.1068-1074 (2009) In Japanese.

[4] J. Itoh, J. Toyosaki, and H. Ohsawa: "High performance V/f control method for PM Motor", IEEJ Trans., Vol.122-D, No.3, pp.253-259 (2002) In Japanese.

[5] H. Yonezawa, K. Taniguchi, T. Morizane and N. Kimura: "Modified Trapezoidal Modulating Signal suitable for PM Synchronous Motor Drives", IEEJ Trans., Vol.125-D, No.1, pp.46-53 (2005) In Japanese.

[6] I. Takahashi and S. Miyairi: "Relation between the Output Voltage Waveform of the PWM Inverter and its Gate Control Signals", IEEJ Trans., Vol.95-B, No.2, pp.73-80 (1975) In Japanese.

[7] I. Takahashi, T. Sekiguchi and S. Miyairi: "Control Method of PWM Inverter Output Wave with Reduced Low Order Harmonic Components", IEEJ Trans., Vol.97-B, No.5, pp.302-308 (1977) In Japanese.

[8] T. Ogura and J. Itoh: "Open Loop Control with a Square Wave Operation and a Total Loss for a Permanent Magnet Motor", JIASC IEEJ, pp.1-101 (2009) In Japanese.

[9] R. Liu, C. Chunting Mi and D. Wenzhong Gao: "Modeling of Eddy-Current Loss of Electrical Machines and Transformers Operated by Pulsewidth-Modulated Inverters", IEEE Trans. Magn., pp.2021-2028 (2008)

[10] M. OGAWA : An Analysis of Transient Phenomena of Magnetizing Current of Transformer Generated by DC Interrupted Excitations

[11] K. Itoh, Y. Hashiba, K. Sakai and T. yagisawa: "The a.c. losses of the rare-earth permanent magnets", IEEJ Trans., Vol.118-A, No.2, pp.182-187 (1998) In Japanese.

[12] R. A. NEWBURY: "Prediction of Loss in Silicon Steel from Distorted Waveforms", IEEE Trans. Magn, pp.262- (1977) In Japanese.